Inorganic Chemistry

Article

pubs.acs.org/IC

Spin Crossover Meets Diarylethenes: Efficient Photoswitching of Magnetic Properties in Solution at Room Temperature

Magdalena Milek, Frank W. Heinemann, and Marat M. Khusniyarov*

Department of Chemistry and Pharmacy, Friedrich-Alexander-Universität Erlangen−Nürnberg, Egerlandstrasse 1, 91058 Erlangen, Germany

Supporting Information

ABSTRACT: A photoisomerizable diarylethene-derived ligand, phen*, has been successfully introduced into a spin-crossover iron(II) complex, [Fe($H_2B(pz)_2)_2$phen*] (**1**; pz =1-pyrazolyl). A ligand-based photocyclization (photocycloreversion) in **1** modifies the ligand field, which, in turn, results in a highly efficient paramagnetic high-spin → diamagnetic low-spin (low-spin → high-spin) transition at the coordinated Fe^{II} ion. The reversible photoswitching of the spin states, and thus the associated magnetic properties, has been performed in solution at room temperature and has been directly monitored by measuring the magnetic susceptibility via the Evans method. The observed spin-state photoconversion in **1** exceeds 40%, which is the highest value for spin-crossover molecular switches in solution at room temperature reported to date. The photoexcited state is extraordinarily thermally stable, showing a half-time of about 18 days in solution at room temperature. Because of the outstanding photophysical properties of diarylethenes, including single-crystalline photochromism, molecular switch **1** may offer a promising platform for controlling the magnetic properties in the solid state and ultimately at the single-molecule level with light at room temperature.

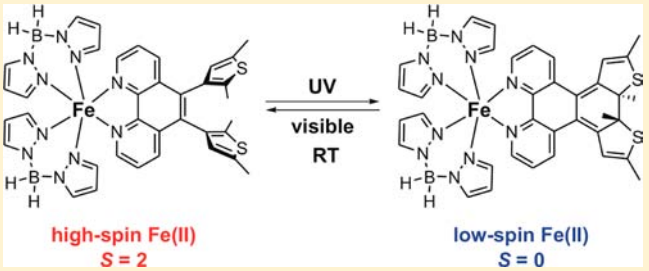

INTRODUCTION

Spin-crossover (SCO) metal complexes are among the best known classes of molecular bistable systems, in which optical, magnetic, and other physicochemical properties can be reversibly switched by changing the temperature, applied pressure, electric and magnetic field, or irradiation with light.[1−13] Although SCO is known for d^4−d^8 first-row transition-metal ions, the most common species are pseudooctahedral d^6 complexes of iron(II), which offer a brilliant opportunity to switch between a diamagnetic low-spin (LS; S = 0) state and a paramagnetic high-spin (HS; S = 2) state via external stimuli. Controlling a molecule's state via *light irradiation* is very attractive because of the extraordinarily high speed of switching, easy and precise addressing, and high selectivity, which suggests application of SCO species as photoswitchable building blocks for molecular electronics and spintronics, communication networks, ultrahigh-density memories, displays, and photosensors.[14−17] Although photoswitching in SCO systems is well documented in a light-induced excited spin-state trapping (LIESST) effect,[18,19] this phenomenon is usually operative at low temperatures, T < 50 K, whereas at higher temperatures, a photoexcited metastable HS state relaxes rapidly back to a LS state, which imposes serious limitations for application of the LIESST effect in genuine photodevices.[20,21]

An interesting approach to switching spin states in SCO complexes with light at room temperature (RT) via a *photoinduced phase transition* has recently been demonstrated by Bousseksou et al.[22,23] However, this effect exists only in a macroscopic phase, i.e., photoswitching of a single molecule is not possible; moreover, the use of pulsed lasers of high intensity is strictly required. On the other hand, a less known ligand-driven light-induced spin-change (LD-LISC) effect[24,25] represents a tempting alternative to the LIESST. Here photoisomerization of a photoactive ligand modifies the ligand field, which, in turn, induces a change of the spin state of a coordinated metal ion, and thus photoswitching can be accomplished at *room temperature*.[26,27] Importantly, unlike the photoinduced phase transition,[22,23] the LD-LISC does not require the presence of a macroscopic phase because it is a natural molecular effect that may allow control of the spin state ultimately at the *single-molecule level*.

Until now, several iron complexes featuring ligands with cis−trans isomerizable −HC═CH− and −N═N− groups were synthesized and photoswitching of the metal spin state via the LD-LISC approach was detected at RT.[27−30] However, the reported cis−trans systems show severe drawbacks: far incomplete ligand photoisomerization, low thermal stability of cis isomers for azo compounds, side photoreactions for −HC═CH− photochromes, irreversibility of photoswitching in the solid state, and generally low spin-state conversion (below 5% in solution). Thus, the known systems are highly inefficient and unreliable, which hinders any possible applications. Con-

Received: July 29, 2013
Published: September 24, 2013

   dx.doi.org/10.1021/ic401960x | *Inorg. Chem.* 2013, 52, 11585−11592

sequently, fundamentally different types of photochromic ligands are needed in order to achieve efficient photoswitching in SCO complexes via the highly promising LD-LISC effect.

In this context, organic photoswitches diarylethenes seem to be very tempting candidates (Scheme 1):[31] Diarylethenes can

Scheme 1. Diarylethene-Based Ligands and Typical Photocyclization and Photocycloreversion Reactions

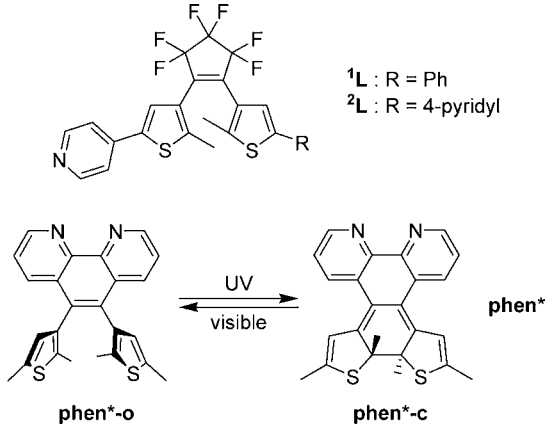

be efficiently and reversibly switched between open- and closed-ring isomers using the light of two significantly different wavelengths, which often leads to nearly complete photoisomerization. Extraordinary resistance to fatigue, outstanding response time for photoisomerization (<10 ps), and the high thermal stability of both isomers[32] render these photochromes highly promising molecular photoswitches for numerous applications.[33−38] Importantly, many diarylethenes undergo reversible photoswitching even in a *single crystalline phase*,[31,32,39] which allows one to control the properties of materials in the solid state. On top of this, photoswitching of diarylethenes at the *single-molecule level* has been demonstrated.[36,40]

Consequently, very recently the first attempts to integrate photoactive diarylethene-based ligands into SCO complexes were independently made by Boillot and Garcia.[41,42] However, photoisomerization of a diarylethene-derived ligand, ^{1}L, in a molecular complex, $[Fe^{1}L_4(NCS)_2]$ (Scheme 1), did not induce a desired spin-state change,[41] whereas photoreaction at ^{2}L in a polymer, $\{Fe^{2}L_2(NCS)_2(MeOH)_2\}_n$, was claimed to result in a metal-to-ligand electron transfer instead of a desired SCO.[42] Thus, so far no evidence for a spin-state change induced by photoisomerization of a diarylethene-based ligand has been provided.

Here we present an iron(II) complex, $[Fe(H_2B(pz)_2)_2phen^*]$ (**1**; pz =1-pyrazolyl), featuring a diarylethene-derived ligand, phen*[43,44] (Scheme 1). In contrast to ^{1}L and ^{2}L, where a metal-coordinating pyridyl unit is attached to a photochrome as a pendant arm, a photoisomerizable site and a metal coordination site are "fused" in phen*.[43,44] The chelating effect and the unique "fused" nature of phen* were both expected to provide a stronger electronic coupling between a coordinated metal ion and the photochrome, which could result in efficient photoswitching of the spin states via ligand-based photoisomerization. Indeed, here we demonstrate that reversible photocyclization/cycloreversion of a diarylethene ligand in **1** does induce reversible photoswitching of the spin states of the coordinated Fe^{II} ion. Photoswitching has been accomplished in solution at RT, and changes of the magnetic properties have been directly detected by measuring the magnetic susceptibility using the Evans method. Integration of the photoisomerizable phen* into **1** allowed us to obtain a very high photoconversion of spin states and an extraordinarily thermally stable photoinduced state. Furthermore, because of the outstanding photophysical properties of diarylethenes,[32] molecular switch **1** may offer a promising platform to control the magnetic properties of solids and ultimately single molecules with light at RT.[45]

EXPERIMENTAL SECTION

Materials. All starting materials and solvents were utilized as received without further purification unless otherwise noted. Pure anhydrous solvents, required for work under an inert gas atmosphere, were gathered from a solid-state solvent purification system by Glass Contour. Dry methanol was obtained by distillation from iodine-activated magnesium under a nitrogen atmosphere. 2,5-Dimethylthien-3-ylboronic acid[46−49] and $K[H_2B(pz)_2]$[50] were prepared according to literature methods; the ligand phen* was prepared by adapting a method from Yam et al.[49]

Instrumentation. Elemental analyses were carried out using an EURO EA analyzer from Eurovector. Electronic absorption spectra were recorded with Shimadzu UV 3600 UV−vis−near-IR and Shimadzu UV-2450 spectrophotometers. The samples were prepared under anaerobic conditions and sealed in QS Quartz Suprasil cells (10 mm light path) with high-vacuum poly(tetrafluoroethylene) spindle valves. NMR spectra were recorded with a JEOL JNM-LA 400 FT NMR spectrometer and processed with *Delta V4.0* software provided by JEOL Ltd. Magnetic susceptibility data in solution were measured using the Evans method[51] in C_7H_8/C_7D_8/tetramethylsilane (TMS) (10:1:1) for variable-temperature measurements and in CH_3CN/CD_3CN (10:1) for photoexperiments. The obtained data were corrected by the temperature dependence of the solvent density. The diamagnetic corrections were determined from Pascal's constants to give $\chi_{dia} = -3.84 \times 10^{-4}$ emu mol^{-1} for **1**.[52]

The temperature-dependent magnetic susceptibility data for **1-o** were simulated using the van't Hoff equation (1), with the equilibrium constant K (2) and ΔH and ΔS as the enthalpy and entropy for SCO, respectively.[30,53]

$$\ln K = -\Delta H/RT + \Delta S/R \quad (1)$$

$$K = \gamma_{HS}/\gamma_{LS} \quad (2)$$

Magnetic susceptibility data of solid samples were collected using a Quantum Design MPMS-XL SQUID magnetometer. Measurements were obtained for a powder restrained within a polycarbonate gel capsule. Direct-current susceptibility data were collected in the temperature range 2−300 K under a magnetic field of 1 T. The program *JulX* was used for simulation and analysis of magnetic susceptibility data.[54] ^{57}Fe Mössbauer spectra were recorded on a WissEl Mössbauer spectrometer (MRG-500) at 77 K and RT in constant-acceleration mode. ^{57}Co/Rh was used as the radiation source. *MFIT* software was used for the quantitative evaluation of the spectral parameters.[55] The temperature of the samples was controlled by an MBBC-HE0106 Mössbauer He/N_2 cryostat within an accuracy of ±0.3 K. Isomer shifts were determined relative to α-iron at 298 K. Monochromatic light sources with λ = 254 nm and power of 8 and 15 W (common lamps for thin-layer chromatography) were used for photocyclization. Halogen lamps of 25 and 50 W were used for photocycloreversion reactions. An LOT-Oriel Xe-OFR arc lamp (1 kW) equipped with an Omni-λ 300 monochromator was used as a wavelength-variable light source.

Synthesis. *$[Fe(H_2B(pz)_2)_2phen^*]$ (1; pz =1-pyrazolyl).* Synthesis was performed under anaerobic conditions using Schlenk techniques. A solution of $K[H_2B(pz)_2]$ (185 mg, 1.0 mmol) in 5 mL of dry methanol was added to a solution of $FeSO_4{\cdot}7H_2O$ (138 mg, 0.5 mmol) in 5 mL of dry methanol and stirred at RT for 10 min. After filtration, a solution of phen* (200 mg, 0.5 mmol) in 15 mL of dry methanol was added dropwise to the filtrate to give a purple solution with a violet powder. The mixture was stored at −35 °C for 2 days

dx.doi.org/10.1021/ic401960x | Inorg. Chem. 2013, 52, 11585−11592

before the precipitate was filtered off and washed with water twice to give **1** as an analytically pure powder (171 mg, 0.23 mmol, 46%). Single crystals suitable for X-ray structure determination were obtained by the slow diffusion of *n*-hexane into a toluene solution of **1**. Elem anal. Calcd for $C_{36}H_{36}B_2FeN_{10}S_2$: C, 57.63; H, 4.84; N, 18.67; S, 8.55. found: C, 58.10; H, 4.87; N, 18.73; S, 8.57.

X-ray Crystallographic Data Collection and Refinement of the Structures. Suitable single crystals were embedded in protective perfluoropolyalkyl ether oil and transferred to the cold nitrogen gas stream of the diffractometer. Intensity data were collected at 100 and 250 K on a Bruker Smart APEX2 diffractometer (Mo Kα radiation, λ = 0.71073 Å, graphite monochromator). Data were corrected for Lorentz and polarization effects; semiempirical absorption corrections were applied on the basis of multiple scans using *SADABS*.[56] The structures were solved by direct methods and refined by full-matrix least-squares procedures on F^2 using *SHELXTL NT 6.12*.[57] All non-H atoms were refined with anisotropic displacement parameters. The H atoms of all compounds were placed in positions of optimized geometry, and their isotropic displacement parameters were tied to those of their corresponding carrier atoms by a factor of 1.2 or 1.5.

One of the dimethylthiophene groups was disordered. Two alternative orientations were refined, resulting in site occupancy factors of 68.3(4) and 31.7(4)% at 100 K and of 70.1(6) and 29.9(6)% at 250 K for the affected atoms S2, C21, C23, C24 and S2A, C21A, C23A, C24A, respectively. The compound crystallized with two molecules of toluene, one of which was disordered. Two alternative orientations were refined that were occupied by 79(1) and 21(1)% at 100 K and by 70(1) and 30(1)% at 250 K for atoms C201−C207 and C211−C217, respectively. FLAT, SIMU, ISOR, and SAME restraints were applied in the refinement of the disordered toluene molecule.

The crystallographic data of the compounds and selected geometrical parameters are listed in Tables 1 and 2, respectively.

Table 1. Crystallographic Data, Data Collection, and Refinement Details for $1{\cdot}2C_7H_8$

	T = 100 K	T = 250 K
chemical formula	$C_{50}H_{52}B_2FeN_{10}S_2$	$C_{50}H_{52}B_2FeN_{10}S_2$
fw	934.61	934.61
cryst size, mm	0.44 × 0.20 × 0.04	0.44 × 0.20 × 0.04
cryst syst	triclinic	triclinic
space group	$P\bar{1}$	$P\bar{1}$
a, Å	13.0663(15)	13.3090(13)
b, Å	15.0234(16)	15.1515(15)
c, Å	15.1226(16)	15.4112(14)
α, deg	63.820(5)	63.665(5)
β, deg	67.216(5)	67.376(5)
γ, deg	66.304(5)	67.038(5)
V, Å^3	2358.5(4)	2478.7(4)
Z	2	2
T, K	100(2)	250(2)
ρ_{calcd}, g cm^{-3}	1.314	1.252
reflns collected/$2\theta_{max}$, deg	24658/52.74	28321/51.36
unique reflns/$I > 2\sigma(I)$	9076/5574	28321/4350
no. of param/restraints	696/103	696/149
λ, Å/μ(Kα), mm^{-1}	0.71073/0.455	0.71073/0.433
R1 [$I > 2\sigma$ (I)]	0.0617	0.0636
wR2/goodness of fit	0.1780/1.017	0.1946/0.962
residual density, e Å^{-3}	+0.569/−0.783	+0.437/−0.609

CCDC 938944 for **1** at 100 K and CCDC 938945 for **1** at 250 K contain the supplementary crystallographic data for this paper. These data can be obtained free of charge from The Cambridge Crystallographic Data Centre via www.ccdc.cam.ac.uk/data_request/cif and also appear as Supporting Information (SI).

Table 2. Selected Bond Distances (Å) and Angles (deg) for $1{\cdot}2C_7H_8$

	T = 100 K	T = 250 K
Fe1−N1	1.967(3)	2.184(3)
Fe1−N2	1.969(3)	2.179(4)
Fe1−N6	1.999(3)	2.144(4)
Fe1−N3	2.002(3)	2.164(4)
Fe1−N7	2.005(3)	2.142(3)
Fe1−N10	2.008(3)	2.173(4)
N2−Fe1−N6	176.14(12)	169.26(13)
N1−Fe1−N7	177.29(12)	171.59(14)
N3−Fe1−N10	178.74(12)	177.91(14)

RESULTS AND DISCUSSION

Synthesis and Crystal Structure. The reaction of phen*[43,44] with $[Fe(H_2B(pz)_2)_2]$, which is generated in situ from $FeSO_4{\cdot}7H_2O$ and $K[H_2B(pz)_2]$,[50] in absolute methanol under anaerobic conditions gives a violet solid of analytically pure **1**. Complex **1** is paramagnetic in solution at RT, as can be judged from broad paramagnetically shifted signals in its ^{1}H NMR spectrum. Recrystallization of **1** from a toluene/*n*-hexane mixture provides X-ray-quality crystals used for crystal structure determination at 100 and 250 K. Species **1** crystallizes in the $P\bar{1}$ space group (Figure 1). Two bis(pyrazolyl)borate(1−) anions

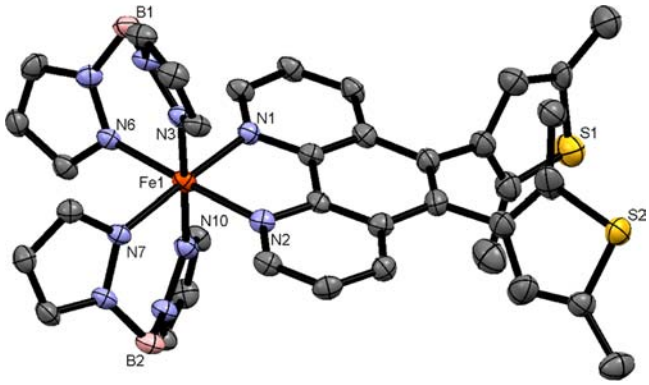

Figure 1. Molecular structure of **1** at T = 100 K. Thermal ellipsoids are drawn at the 50% probability level, the H atoms are omitted for clarity, and the antiparallel conformation of a diarylethene-based ligand is shown.

and one neutral phen* ligand form a distorted octahedral N_6 coordination environment around an Fe^{II} center. All Fe−N bond distances are long [2.179(4) and 2.184(3) Å with phen* and 2.142(3)−2.173(4) Å with $H_2B(pz)_2$ anions], confirming a HS Fe^{II} ion (S = 2) present in the solid state at 250 K (Table 2).[58,59] The coordinated phen* presents simultaneously in two conformations:[31] parallel (29.9%) and antiparallel (70.1%), reflected by the disorder of one dimethylthiophene group in the crystal (see the SI for a parallel conformer).[60] Two five-membered thiophene rings in the antiparallel conformer form dihedral angles of 65.2 and 74.5° with a nearly planar phenanthroline unit at 250 K (66.9 and 74.5° in the parallel conformer). Thus, the π systems of the two thiophene groups and the phenanthroline backbone are essentially electronically uncoupled.

The same crystal measured at 100 K provides similar but not identical geometric parameters for **1** (Table 2). The two

dx.doi.org/10.1021/ic401960x | *Inorg. Chem.* 2013, 52, 11585−11592

thiophene rings form dihedral angles of 61.8 and 72.6° with the phenanthroline plane in the antiparallel conformer and 64.4 and 72.6° in the parallel conformer. Although all above-mentioned dihedral angles are slightly reduced at 100 K compared with a 250 K structure, the π systems of the two thiophene units and the phenanthroline are still substantially uncoupled at 100 K. Importantly, all Fe−N bond distances shrink considerably to 1.969(3) and 1.967(3) Å with phen* and 1.999(3)−2.008(3) Å with $H_2B(pz)_2$ anions at 100 K. Such dramatic changes of the Fe−N bond distances are typical for a thermally induced LS $Fe^{II}(S = 0) \leftrightarrow$ HS $Fe^{II}(S = 2)$ transition.[58,59]

Spectroscopic and Magnetochemical Studies. Indeed, temperature-dependent magnetic susceptibility measurements performed on a microcrystalline sample of **1** confirm a thermally induced spin transition: The effective magnetic moment μ_{eff} of 5.23 μ_B is nearly constant in the temperature range 210−300 K, which corroborates a pure HS Fe^{II} state (Figure 2). At temperatures below 210 K, μ_{eff} decreases

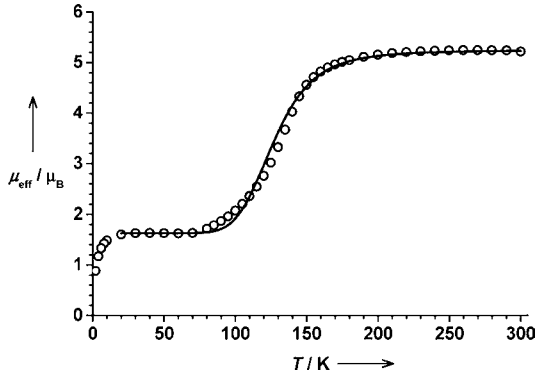

Figure 2. Temperature-dependent effective magnetic moment of **1** measured on a microcrystalline sample at an external magnetic field of 1 T. Fit parameters: enthalpy ΔH = 10.2(4) kJ mol^{-1}, entropy ΔS = 76(3) J K^{-1} mol^{-1}, and transition temperature $T_{1/2}$ = 135(5) K. See the SI for other parameters.

gradually, disclosing a HS → LS transition with $T_{1/2}$ = 135 K, and reaches a second plateau of 1.62 μ_B at 20−70 K with a residual HS fraction of 10%. The residual HS fraction varies between 10 and 15% for independently synthesized and dried samples and is likely due to a small amount of solvent molecules remaining in the dried samples. Finally, at temperatures below 20 K, μ_{eff} decreases further, reaching 0.88 μ_B at 2 K, which is ascribed to a zero-field-splitting effect on a residual HS fraction.

Temperature-dependent zero-field ^{57}Fe Mössbauer spectroscopy performed on microcrystalline **1** confirms SCO in the solid state: A single quadrupole doublet with a high isomer shift δ = 1.01 mm s^{-1} and a quadrupole splitting $|\Delta E_Q|$ = 1.77 mm s^{-1} points unambiguously to a HS Fe^{II} complex as the only iron-containing species present in the sample of **1** at RT (Figure 3).[61,62] Upon cooling to T = 77 K, the former signal becomes slightly shifted to δ = 1.14 mm s^{-1} because of a second-order Doppler shift[62] and the quadrupole splitting becomes as large as 2.51 mm s^{-1}. More importantly, a new quadrupole doublet appears with a relative intensity of 89%, which is characterized by a lower isomer shift δ = 0.50 mm s^{-1} and a much smaller quadrupole splitting $|\Delta E_Q|$ = 0.48 mm s^{-1}. The latest signal is very characteristic for a LS Fe^{II} ion in a pseudooctahedral environment.[61−63] Thus, a thermally induced

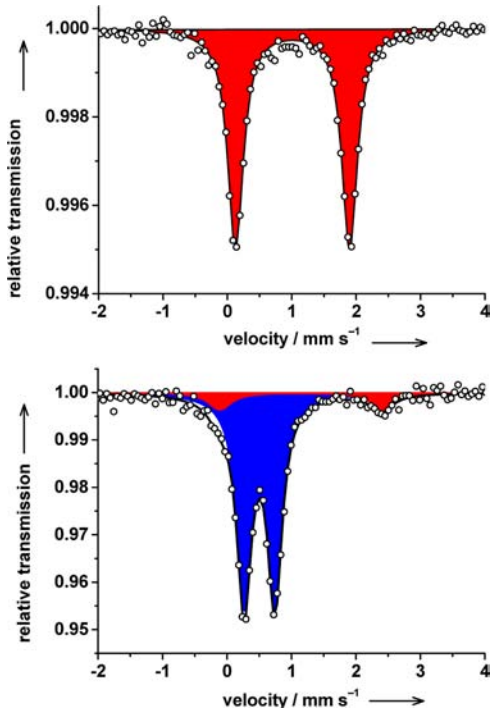

Figure 3. Zero-field ^{57}Fe Mössbauer spectra of a powder sample of **1** recorded at 298 K (top) and 77 K (bottom). Fit parameters: (top) HS Fe^{II}, δ = 1.01 mm s^{-1}, $|\Delta E_Q|$ = 1.77 mm s^{-1}, relative intensity 100%; (bottom) (a) HS Fe^{II}, δ = 1.14 mm s^{-1}, $|\Delta E_Q|$ = 2.51 mm s^{-1}, relative intensity 11%, in red; (b) LS Fe^{II}, δ = 0.50 mm s^{-1}, $|\Delta E_Q|$ = 0.48 mm s^{-1}, relative intensity 89%, in blue.

HS ↔ LS transition in **1** has been disclosed by temperature-dependent X-ray crystallography, magnetic susceptibility measurements, and Mössbauer spectroscopy in the solid state. Because we study the photomagnetic properties of **1** in solution (vide infra), it is important to investigate the electronic structure of the complex in solution, which might, in principle, differ from that in the solid state.

The electronic absorption spectrum of **1** recorded in MeCN at RT shows two very intense bands in the 200−300 nm region and a broad shoulder at about 340 nm, which are bathochromically shifted relative to the corresponding bands of the metal-free phen* (see the SI). Additionally, a weaker broad band centered at about 550 nm is detected for **1**, which can be assigned to a metal-to-ligand charge-transfer transition.[64] In agreement with the data obtained for similar complexes,[64] no additional bands between 700 and 1500 nm could be observed for **1**. Note that, using UV−vis spectroscopy, no evidence for dissociation of the chelating phen* in solution was found when toluene or MeCN was employed as the solvent: **1** was found to be stable in a deoxygenated dry MeCN solution in the dark for weeks. In contrast, the use of methanol as the solvent resulted in poor reproducible UV−vis spectra and partial dissociation of the complex in as-prepared and irradiated solutions.

The magnetic properties of **1** in solution were investigated by temperature-dependent ^{1}H NMR spectroscopy using the Evans method.[65,66] The effective magnetic moment of **1** in a toluene solution at RT is 5.31 μ_B, remaining nearly constant upon cooling to 250 K (Figure 4), which is in agreement with a HS Fe^{II} state in solution within a given temperature range. At temperatures below 250 K, μ_{eff} decreases gradually to 4.30 μ_B determined at T = 188 K. The temperature-dependent μ_{eff} was

dx.doi.org/10.1021/ic401960x | Inorg. Chem. 2013, 52, 11585−11592

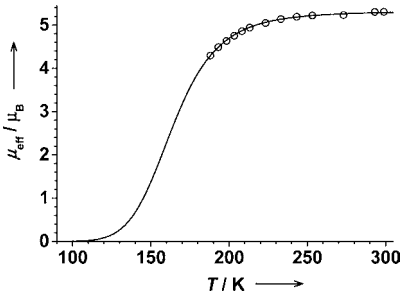

Figure 4. Temperature-dependent effective magnetic moment of **1** in a toluene solution determined by ^{1}H NMR spectroscopy using the Evans method (toluene/toluene-d_8/TMS = 10/1/1). Fit parameters: ΔH = 15.3(1) kJ mol^{-1}, ΔS = 93.4(6) J K^{-1} mol^{-1}, and $T_{1/2}$ = 164(1) K.

fitted using the van't Hoff equation,[30] providing good estimations for the thermodynamic parameters of SCO in solution: enthalpy ΔH = 15.3(1) kJ mol^{-1}, entropy ΔS = 93.4(6) J K^{-1} mol^{-1}, and transition temperature $T_{1/2}$ = 164(1) K. The obtained thermodynamic parameters are typical for iron(II) SCO systems.[30,53] Intermolecular interactions present in the solid state but absent in solution yield slightly differing thermodynamic parameters for SCO and shifted transition temperatures in solution and in the solid state. Overall, a thermally driven HS ↔ LS transition in **1** occurs in both the solid state and solution, justifying that the HS and LS states are energetically close. Hence, small changes of the ligand field induced via ligand-based photoisomerization could indeed result in a spin-state change in **1**.

Photophysical Studies. Prior to investigating the photophysical properties of **1**, we examined the photochemistry of the metal-free phen* under conditions similar to those used for **1**. Thus, irradiation of phen* at λ = 254 nm for 45 s in MeCN results in the decreasing intensity of the bands at 232 and 267 nm accompanied by the appearance of a new intense band at 362 nm with a shoulder and a moderately intense band at about 520 nm (Figure 5). These changes are characteristic for ligand photocyclization: phen*-o → phen*-c (Scheme 1). Similar observations were made by Yam et al. under slightly different conditions in benzene.[43,44] The photostationary state is characterized by the presence of 60% of phen*-c and 40% of phen*-o, as determined by NMR spectroscopy. The photocyclization is reversible: by irradiation of a MeCN solution of phen*-c with visible light for 55 s, the closed-ring isomer undergoes photocycloreversion phen*-c → phen*-o and the initial UV−vis spectrum of phen*-o is restored (see the SI). In the dark, the closed-ring isomer slowly thermally relaxes to the open-ring ground state: the half-life of phen*-c in a MeCN solution at RT is estimated at 137 h (~5.7 days; see the SI).

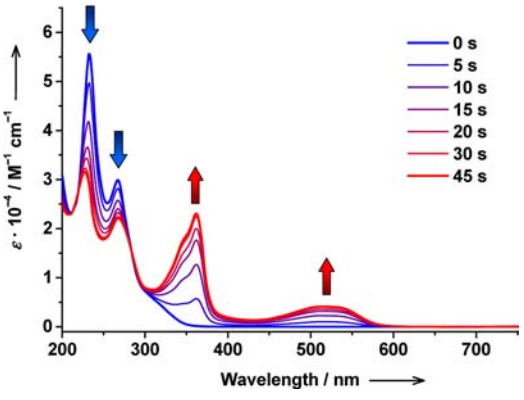

Figure 5. Photoresponse of phen*-o to λ = 254 nm irradiation (8 W, MeCN solution, and c = 6 × 10^{-5} M) detected by UV−vis spectroscopy showing photocyclization phen*-o → phen*-c.

In the next step, we irradiated a *diluted* solution of **1** in MeCN with UV light at RT and monitored the changes by UV−vis spectroscopy. Two absorption bands at 233 and 275 nm decrease in intensity, and a new strong band at 376 nm and a weaker broad band at about 545 nm emerge upon irradiation at λ = 254 nm for 4 min (Figure 6). No absorption bands above

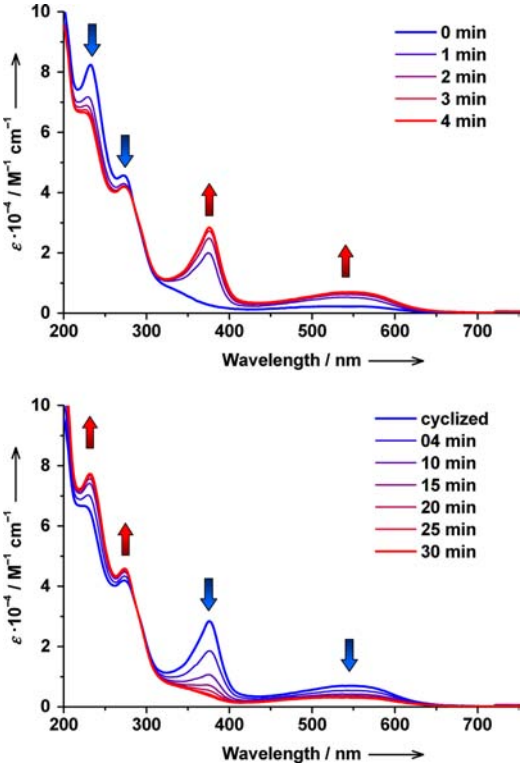

Figure 6. Photocyclization of **1** induced by UV light (λ = 254 nm, 23 W, MeCN solution, and c = 1.33 × 10^{-5} M; top) and the corresponding photocycloreversion induced by visible light (λ > 400 nm, halogen lamp, 25 W, MeCN solution, and c = 1.33 × 10^{-5} M; bottom) detected by UV−vis spectroscopy at RT.

700 and below 1500 nm were observed. These changes resemble those observed for photocyclization of the metal-free ligand: phen*-o → phen*-c. However, the new bands in **1** (376 and 545 nm) are significantly bathochromically shifted compared to the bands of the metal-free phen*-c (361 and 514 nm; see the SI). Thus, the metal-coordinated phen* undergoes photocyclization in **1** and remains coordinated: **1-o** → **1-c**. The photostationary state is approximately composed of 70% of **1-c** and 30% of **1-o**, as could be estimated by comparing the intensity of the prominent absorption band at 376 nm with that of the corresponding band of phen*-c. The photocyclization in **1** can be induced by excitations at λ = 242 ± 8 or 276 ± 8 nm as well; however, in later cases, photocyclization proceeds slower with the light sources at hand (see the SI). The rate of photocyclization in **1** is reduced compared to the metal-free phen*, as is often observed for metal-coordinated photoisomerizable ligands.[67] It is important to note that no

dx.doi.org/10.1021/ic401960x | Inorg. Chem. 2013, 52, 11585−11592

evidence for photodissociation of phen* was found in MeCN. However, exposure of a MeOH solution of **1** to UV light resulted in the partial photodissociation and formation of the metal-free phen*, as detected by UV−vis spectroscopy.

The photocyclization in **1** is reversible: the corresponding photocycloreversion **1-c** → **1-o** can be induced by selective irradiation into new bands at 376 or 545 nm or by exposure to visible light (Figure 6). Irradiation of **1-c** at λ = 376 ± 8 nm leads to a nearly complete photocycloreversion and recovery of the initial UV−vis spectrum of **1-o**, whereas the use of visible light results in a slightly less complete cycloreversion. In the dark, the closed-ring isomer **1-c** slowly thermally relaxes to the open-ring form **1-o**: the half-life of **1-c** in a MeCN solution at RT is estimated at 421 h (~18 days). Reversible photoswitching **1-o** ↔ **1-c** can be accomplished several times, as can be best monitored by following the prominent absorption band at 376 nm (Figure 7): Alternate irradiation with λ = 254 nm

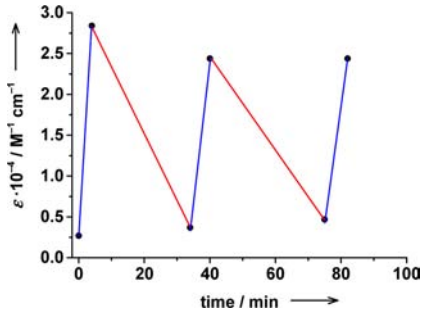

Figure 7. Multiple photoswitching of **1** at RT detected by monitoring the absorption at 376 nm in the UV−vis spectrum (MeCN solution and $c = 1.33 \times 10^{-5}$ M). Photocyclization: λ = 254 nm, 23 W, blue line. Photocycloreversion: visible light (λ > 400 nm), halogen lamp, 25 W, red line.

and visible light results in alternating increases and decreases of absorption, which corresponds to photocyclization and photocycloreversion processes, respectively.

The crucial question of this work to be answered is whether the ligand-based photocyclization **1-o** → **1-c** produces changes to the ligand field large enough to induce a spin transition at the coordinated metal ion. To answer this question, we performed bulk photolysis of a *concentrated* solution of **1** in MeCN/MeCN-d_3. During irradiation at λ = 254 nm, small amounts of solution were withdrawn to monitor the magnetic properties by ^{1}H NMR spectroscopy using the Evans method,[65,66] whereas the photocyclization process and the stability of the complex were followed by UV−vis spectroscopy in solution after appropriate dilution. The magnetic moment of **1** in an acetonitrile solution prior to irradiation is 5.25 μ_B, which corresponds to a pure HS Fe^{II} state. Upon irradiation with UV light, μ_{eff} decreases slowly, reaching a value of 3.16 μ_B after 42 h (Figure 8). The latest value corresponds to approximately 60% of HS Fe^{II} and 40% of LS Fe^{II} species present in the irradiated solution.

UV−vis monitoring of the photoreaction in the bulk photolysis experiment reveals a much slower photocyclization compared to the previous experiments on highly diluted solutions (Figures 6 and 7): **1-o** → **1-c** photoconversion of about 40% was determined by UV−vis spectroscopy after 42 h of irradiation in the bulk photolysis experiment (see the SI). The increased time required for photocyclization in the bulk photolysis experiment is due to a much higher amount/

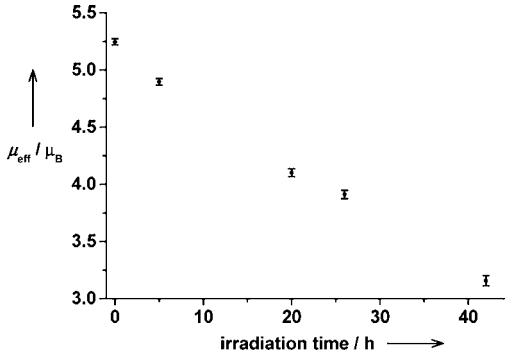

Figure 8. Evolution of the effective magnetic moment of **1** exposed to UV irradiation in the bulk photolysis experiment at RT, as determined using the Evans method (λ = 254 nm, 23 W, solution in MeCN/MeCN-d_3 = 10/1, and $c = 4.9 \times 10^{-4}$ M).

concentration of **1** and the penetration depth limit for UV light in the concentrated solution in bulk photolysis. Prolonged UV irradiation (t > 42 h) leads to the gradual decomposition of **1**, as was observed by monitoring via UV−vis spectroscopy.

Thus, a photoinduced ligand-based cyclization is accompanied by a metal-based SCO in solution at RT. The metal-based HS → LS conversion of about 40% determined by the Evans method is in excellent agreement with a ligand-based photocyclization **1-o** → **1-c** conversion of about 40%, as confirmed by UV−vis spectroscopy. Hence, every ligand-based photocyclization event is roughly accompanied by a spin transition at one Fe^{II} ion. The spin-state conversion for **1** is 40%, which is the highest reported value for photoswitchable SCO systems detected in solution at RT. For comparison, the maximum spin-state conversion reported by Nishihara et al. in solution is 3%.[28]

Note that open-ring diarylethenes are generally present in solution as two conformers: antiparallel and parallel (typical ratio 1:1) being in equilibrium.[31] Usually fast interconversion of the conformers in solution is significantly slowed in the case of phen* because of hindered rotation of the thiophene groups.[43] Only the antiparallel conformer is photoactive, whereas the parallel conformer is photoinactive because of Woodward−Hoffmann rules.[31,68,69] Thus, only a fraction of **1-o** bearing the antiparallel conformer of phen*-o is photoactive. In the crystalline phase, the ratio of antiparallel/parallel is 7:3 (vide supra). In solution, this ratio is not known; however, both antiparallel and parallel conformers are likely to be present. Therefore, photoconversion corrected to the amount of photoactive species is likely to exceed 40% (up to 100% for antiparallel/parallel = 4/6).

Photoswitching of the spin states in **1** is reversible: To test the reversibility, a solution of **1-o** was irradiated at λ = 254 nm for 20 h, which led to partial photocyclization and a concomitant decrease of μ_{eff} from 5.45 to 4.68 μ_B (Figure 9). Upon further irradiation of the sample with visible light for 7 h, photocycloreversion **1-c** → **1-o** led to the partial restoration of μ_{eff} to the value of 4.93 μ_B. The complete restoration of the magnetic moment could not be achieved because of incomplete photocycloreversion with visible light. The photocyclization and concomitant HS → LS photoswitching can be repeated, as demonstrated by a second irradiation with UV light (Figure 9).

The open-ring isomer phen*-o cannot be planar for steric reasons (Scheme 1). Thus, the π system of the phenanthroline backbone and the π systems of the two thiophenes are essentially electronically uncoupled in phen*-o. Photocycliza-

dx.doi.org/10.1021/ic401960x | Inorg. Chem. 2013, 52, 11585−11592

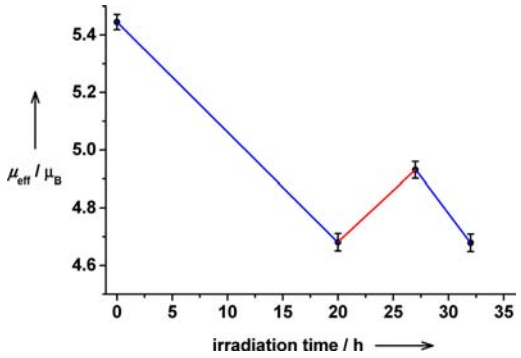

Figure 9. Multiple photoswitching of the effective magnetic moment of **1** detected by the Evans method in the bulk photolysis experiment at RT (solution in MeCN/MeCN-d_3 = 10/1 and $c = 4.9 \times 10^{-4}$ M). Photocyclization: λ = 254 nm, 23 W, blue line. Photocycloreversion: visible light (λ > 400 nm), halogen lamp, 25 W, red line.

tion of the ligand results in the formation of a new C−C bond in phen*-c. At the same time, phen*-c becomes nearly planar and a common π system comprising the phenanthroline and two thiophene units is built. This extended π system is expected to render phen*-c a better π acceptor than phen*-o. Hence, a stronger π-acceptor phen*-c produces a stronger ligand field, which stabilizes a LS Fe^{II} in **1-c**, whereas a weaker π-acceptor phen*-o produces a weaker ligand field, which stabilizes a HS Fe^{II} in **1-o**. Consequently, reversible ligand photoisomerization phen*-o ↔ phen*-c allows us to switch reversibly between the paramagnetic HS and diamagnetic LS states of the Fe^{II} ion in **1** by light in solution at RT.

Comments on a Recent Publication by Oshio et al.[70]

During the final stage of the preparation of the original manuscript, a closely related work by Oshio et al. appeared.[70] The authors reported the synthesis of the same complex **1** and investigated its photophysical properties. In their work, Oshio et al. obtained crystals of **1** featuring only a photoinactive parallel conformer,[70] which prevents photocyclization and thus possible photoswitching of the magnetic properties in the solid state at RT. Using another solvent for crystallization, we obtained another polymorph of **1** that contains a photoactive antiparallel conformer (vide supra), which makes photoswitching in the solid state feasible. More importantly, using butyronitrile as the solvent and UV−vis spectroscopy as an indirect probe for the spin state, Oshio and co-workers reported photoswitching of the spin states only at low temperatures (estimated spin-state photoconversion of 20% at 173 K). Photoswitching of the magnetic properties *at RT was not achieved* by Oshio's group (see Figure 5 in their paper[70])! However, in our work, using acetonitrile as the solvent and NMR spectroscopy (Evans method) as a direct probe for the spin state, we revealed a reversible and highly efficient (>40%) photoswitching of the spin states at RT!

CONCLUSIONS

A photoactive diarylethene-based ligand, phen*, was successfully introduced into a SCO iron(II) complex, **1**, to allow photocontrol of the metal spin state via ligand photoisomerization. Both the chelating effect and the unique "fused" nature of phen* likely contribute to the highest spin-state conversion (>40%) detected for SCO systems in solution at RT reported to date. Unlike the LIESST effect, which yields photoexcited states with common half-times on the order of nanoseconds at RT,[71,72] the half-time of the photoexcited state in the molecular switch **1** in solution is estimated at 18 days at RT. Overall, successful integration of the diarylethene ligand into the SCO complex **1** may open a great opportunity to efficiently and reversibly switch the magnetic properties of solids, thin films, and at single-molecule level[11−13,36,64,73−78] *with light at RT*, which could find diverse applications in molecular electronics and spintronics. Photoswitching of the magnetic properties of **1** in the solid state and the single-crystalline phase is currently under investigation in our group.

ASSOCIATED CONTENT

Supporting Information

Additional electronic absorption spectra and magnetic data, thermal relaxation curves, and crystallographic data including CIF files. This material is available free of charge via the Internet at http://pubs.acs.org.

AUTHOR INFORMATION

Corresponding Author

*E-mail: marat.khusniyarov@chemie.uni-erlangen.de. Tel.: +49(0)9131 8527464. Fax: +49(0)9131 8527367.

Notes

The authors declare no competing financial interest.

ACKNOWLEDGMENTS

The Fonds der Chemischen Industrie (Liebig Fellowship for M.M.K.) and the Deutsche Forschungsgemeinschaft (DFG Research Grant KH 279/2-1) are acknowledged for financial support. M.M. is grateful to the FAU Graduate School for a stipend. Friedrich-Alexander-Universität Erlangen−Nürnberg and Lehrstuhl für Anorganische und Allgemeine Chemie (Prof. Karsten Meyer) are acknowledged for general support.

REFERENCES

(1) Gütlich, P.; Goodwin, H. A. *Spin Crossover in Transition Metal Compounds I−III, Topics in Current Chemistry*; Springer-Verlag: Berlin, 2004; Vols. *233*−*235*.
(2) Halcrow, M. A. *Spin-Crossover Materials, Properties and Applications*; John Wiley & Sons, Ltd.: New York, 2013.
(3) *Eur. J. Inorg. Chem.* **2013**, Special Issue, 574−1067.
(4) Gütlich, P.; Gaspar, A. B.; Garcia, Y. *Beilstein J. Org. Chem.* **2013**, *9*, 342−391.
(5) Roubeau, O. *Chem.—Eur. J.* **2012**, *18*, 15230−15244.
(6) Hayami, S.; Komatsu, Y.; Shimizu, T.; Kamihata, H.; Lee, Y. H. *Coord. Chem. Rev.* **2011**, *255*, 1981−1990.
(7) Gass, I. A.; Batten, S. R.; Forsyth, C. M.; Moubaraki, B.; Schneider, C. J.; Murray, K. S. *Coord. Chem. Rev.* **2011**, *255*, 2058−2067.
(8) Bousseksou, A.; Molnar, G.; Salmon, L.; Nicolazzi, W. *Chem. Soc. Rev.* **2011**, *40*, 3313−3335.
(9) Munoz, M. C.; Real, J. A. *Coord. Chem. Rev.* **2011**, *255*, 2068−2093.
(10) Olguin, J.; Brooker, S. *Coord. Chem. Rev.* **2011**, *255*, 203−240.
(11) Meded, V.; Bagrets, A.; Fink, K.; Chandrasekar, R.; Ruben, M.; Evers, F.; Bernand-Mantel, A.; Seldenthuis, J. S.; Beukman, A.; van der Zant, H. S. J. *Phys. Rev. B* **2011**, *83*, 245415.
(12) Gopakumar, T. G.; Matino, F.; Naggert, H.; Bannwarth, A.; Tuczek, F.; Berndt, R. *Angew. Chem., Int. Ed.* **2012**, *51*, 6262−6266.
(13) Miyamachi, T.; Gruber, M.; Davesne, V.; Bowen, M.; Boukari, S.; Joly, L.; Scheurer, F.; Rogez, G.; Yamada, T. K.; Ohresser, P.; Beaurepaire, E.; Wulfhekel, W. *Nat. Commun.* **2012**, *3*, 938.
(14) Létard, J.-F.; Guionneau, P.; Goux-Capes, L. *Top. Curr. Chem.* **2004**, *235*, 221−249.
(15) Kahn, O.; Martinez, C. J. *Science* **1998**, *279*, 44−48.

(16) Garcia, Y.; Ksenofontov, V.; Gütlich, P. *Hyperfine Interact.* **2002**, *139*−*140*, 543−551.
(17) Sato, O.; Tao, J.; Zhang, Y.-Z. *Angew. Chem., Int. Ed.* **2007**, *46*, 2152−2187.
(18) Decurtins, S.; Gütlich, P.; Köhler, C. P.; Spiering, H.; Hauser, A. *Chem. Phys. Lett.* **1984**, *105*, 1−4.
(19) Hauser, A. *Top. Curr. Chem.* **2004**, *234*, 155−198.
(20) Létard, J.-F.; Guionneau, P.; Nguyen, O.; Costa, J. S.; Marcén, S.; Chastanet, G.; Marchivie, M.; Goux-Capes, L. *Chem.—Eur. J.* **2005**, *11*, 4582−4589.
(21) Halcrow, M. A. *Chem. Soc. Rev.* **2008**, *37*, 278−289.
(22) Bonhommeau, S.; Molnár, G.; Galet, A.; Zwick, A.; Real, J.-A.; McGarvey, J. J.; Bousseksou, A. *Angew. Chem., Int. Ed.* **2005**, *44*, 4069−4073.
(23) Cobo, S.; Ostrovskii, D.; Bonhommeau, S.; Vendier, L.; Molnar, G.; Salmon, L.; Tanaka, K.; Bousseksou, A. *J. Am. Chem. Soc.* **2008**, *130*, 9019−9024.
(24) Zarembowitch, J.; Roux, C.; Boillot, M.-L.; Claude, R.; Itie, J.-P.; Polian, A.; Bolte, M. *Mol. Cryst. Liq. Cryst.* **1993**, *234*, 247−254.
(25) Boillot, M.-L.; Roux, C.; Audiere, J.-P.; Dausse, A.; Zarembowitch, J. *Inorg. Chem.* **1996**, *35*, 3975−3980.
(26) Boillot, M.-L.; Chantraine, S.; Zarembowitch, J.; Lallemand, J. Y.; Prunet, J. *New J. Chem.* **1999**, *23*, 179−183.
(27) Boillot, M.-L.; Zarembowitch, J.; Sour, A. *Top. Curr. Chem.* **2004**, *234*, 261−276.
(28) Hasegawa, Y.; Kume, S.; Nishihara, H. *Dalton Trans.* **2009**, 280−284.
(29) Hasegawa, Y.; Takahashi, K.; Kume, S.; Nishihara, H. *Chem. Commun.* **2011**, *47*, 6846−6848.
(30) Takahashi, K.; Hasegawa, Y.; Sakamoto, R.; Nishikawa, M.; Kume, S.; Nishibori, E.; Nishihara, H. *Inorg. Chem.* **2012**, *51*, 5188−5198.
(31) Irie, M. *Chem. Rev.* **2000**, *100*, 1685−1716.
(32) Irie, M. *Photochem. Photobiol. Sci.* **2010**, *9*, 1535−1542.
(33) Raymo, F. M.; Tomasulo, M. *Chem. Soc. Rev.* **2005**, *34*, 327−336.
(34) Tian, H.; Wang, S. *Chem. Commun.* **2007**, 781−792.
(35) Zhang, J.; Zou, Q.; Tian, H. *Adv. Mater.* **2013**, *25*, 378−399.
(36) Irie, M.; Fukaminato, T.; Sasaki, T.; Tamai, N.; Kawai, T. *Nature* **2002**, *420*, 759−760.
(37) Kobatake, S.; Takami, S.; Muto, H.; Ishikawa, T.; Irie, M. *Nature* **2007**, *446*, 778−781.
(38) Irie, M.; Kobatake, S.; Horichi, M. *Science* **2001**, *291*, 1769−1772.
(39) Morimoto, M.; Irie, M. *Chem. Commun.* **2005**, 3895−3905.
(40) Fukaminato, T.; Sasaki, T.; Kawai, T.; Tamai, N.; Irie, M. *J. Am. Chem. Soc.* **2004**, *126*, 14843−14849.
(41) Sénéchal-David, K.; Zaman, N.; Walko, M.; Halza, E.; Rivière, E.; Guillot, R.; Feringa, B. L.; Boillot, M.-L. *Dalton Trans.* **2008**, 1932−1936.
(42) Garcia, Y.; Ksenofontov, V.; Lapouyade, R.; Naik, A. D.; Robert, F.; Gütlich, P. *Opt. Mater.* **2011**, *33*, 942−948.
(43) Yam, V. W.-W.; Ko, C.-C.; Zhu, N. *J. Am. Chem. Soc.* **2004**, *126*, 12734−12735.
(44) Ko, C.-C.; Kwok, W.-M.; Yam, V. W.-W.; Phillips, D. L. *Chem.—Eur. J.* **2006**, *12*, 5840−5848.
(45) Šalitroš, I.; Madhu, N. T.; Boča, R.; Pavlik, J.; Ruben, M. *Monatsh. Chem.* **2009**, *140*, 695−733.
(46) Ivanov, S. N.; Lichitskii, B. V.; Dudinov, A. A.; Martynkin; Krayushkin, M. M. *Chem. Heterocycl. Compd.* **2001**, *37*, 85−90.
(47) D. Peeters, L.; G. Jacobs, S.; Eevers, W.; J. Geise, H. *Tetrahedron* **1994**, *50*, 11533−11540.
(48) Nikitidis, G.; Gronowitz, S.; Hallberg, A.; Staalhandske, C. *J. Org. Chem.* **1991**, *56*, 4064−4066.
(49) Ko, C.-C.; Kwok, W.-M.; Yam, V.; Phillips, D. *Chem.—Eur. J.* **2006**, *12*, 5840−5848.
(50) Hill, A.; Malget, J.; White, A.; Williams, D. *Eur. J. Inorg. Chem.* **2004**, 818−828.
(51) Evans, D. F. *J. Chem. Soc.* **1959**, 2003−2005.
(52) Bain, G.; Berry, J. *J. Chem. Educ.* **2008**, *85*, 532.
(53) Weber, B.; Walker, F. A. *Inorg. Chem.* **2007**, *46*, 6794−6803.
(54) Bill, E. *JulX*, version 1.5; MPI for Bioinorganic Chemistry: Muelheim/Ruhr, Germany, 2008.
(55) Bill, E. *MFIT*, version 1.1; MPI for Bioinorganic Chemistry: Muelheim/Ruhr, Germany, 2008.
(56) *SADABS 2008/1*; Bruker AXS, Inc.: Madison, WI, 2009.
(57) Sheldrick, G. M. *Acta Crystallogr., Sect. A* **2008**, *64*, 112−122.
(58) Real, J. A.; Munoz, M. C.; Faus, J.; Solans, X. *Inorg. Chem.* **1997**, *36*, 3008−3013.
(59) Thompson, A. L.; Goeta, A. E.; Real, J. A.; Galet, A.; Munoz, M. C. *Chem. Commun.* **2004**, 1390−1391.
(60) The given numbers are the corresponding site occupancy factors as determined for a 250 K structure. The factors for a 100 K structure are slightly different: 31.7 and 68.3% for parallel and antiparallel conformers, respectively.
(61) Moliner, N.; Salmon, L.; Capes, L.; Munoz, M. C.; Letard, J.-F.; Bousseksou, A.; Tuchagues, J.-P.; McGarvey, J. J.; Dennis, A. C.; Castro, M.; Burriel, R.; Real, J. A. *J. Phys. Chem. B* **2002**, *106*, 4276−4283.
(62) Gütlich, P.; Bill, E.; Trautwein, A. X. *Mössbauer Spectroscopy and Transition Metal Chemistry*; Springer-Verlag: Berlin: 2011.
(63) Khusniyarov, M. M.; Weyhermüller, T.; Bill, E.; Wieghardt, K. *Angew. Chem., Int. Ed.* **2008**, *47*, 1228−1231.
(64) Naggert, H.; Bannwarth, A.; Chemnitz, S.; von Hofe, T.; Quandt, E.; Tuczek, F. *Dalton Trans.* **2011**, *40*, 6364−6366.
(65) Evans, D. F. *J. Chem. Soc.* **1959**, 2003−2005.
(66) Schubert, E. M. *J. Chem. Educ.* **1992**, *69*, 62.
(67) Kume, S.; Nishihara, H. *Dalton Trans.* **2008**, 3260−3271.
(68) Woodward, R. B.; Hoffmann, R. *J. Am. Chem. Soc.* **1965**, *87*, 395−397.
(69) Longuet-Higgins, H. C.; Abrahamson, E. W. *J. Am. Chem. Soc.* **1965**, *87*, 2045−2046.
(70) Nihei, M.; Suzuki, Y.; Kimura, N.; Kera, Y.; Oshio, H. *Chem.—Eur. J.* **2013**, *19*, 6946−6949.
(71) McCusker, J. K.; Rheingold, A. L.; Hendrickson, D. N. *Inorg. Chem.* **1996**, *35*, 2100−2112.
(72) Stock, P.; Pędziński, T.; Spintig, N.; Grohmann, A.; Hörner, G. *Chem.—Eur. J.* **2013**, *19*, 839−842.
(73) Alam, M. S.; Stocker, M.; Gieb, K.; Müller, P.; Haryono, M.; Student, K.; Grohmann, A. *Angew. Chem., Int. Ed.* **2010**, *49*, 1159−1163.
(74) Bernien, M.; Wiedemann, D.; Hermanns, C. F.; Krüger, A.; Rolf, D.; Kroener, W.; Müller, P.; Grohmann, A.; Kuch, W. *J. Phys. Chem. Lett.* **2012**, *3*, 3431−3434.
(75) Cavallini, M.; Bergenti, I.; Milita, S.; Ruani, G.; Salitros, I.; Qu, Z. R.; Chandrasekar, R.; Ruben, M. *Angew. Chem., Int. Ed.* **2008**, *47*, 8596−8600.
(76) Palamarciuc, T.; Oberg, J. C.; El Hallak, F.; Hirjibehedin, C. F.; Serri, M.; Heutz, S.; Letard, J.-F.; Rosa, P. *J. Mater. Chem.* **2012**, *22*, 9690−9695.
(77) Warner, B.; Oberg, J. C.; Gill, T. G.; El Hallak, F.; Hirjibehedin, C. F.; Serri, M.; Heutz, S.; Arrio, M.-A.; Sainctavit, P.; Mannini, M.; Poneti, G.; Sessoli, R.; Rosa, P. *J. Phys. Chem. Lett.* **2013**, *4*, 1546−1552.
(78) Pronschinske, A.; Chen, Y.; Lewis, G. F.; Shultz, D. A.; Calzolari, A.; Buongiorno Nardelli, M.; Dougherty, D. B. *Nano Lett.* **2013**, *13*, 1429−1434.